ELSEVIER

Solar Energy Materials and Solar Cells 46 (1997) 1–16

Solar Energy Materials and Solar Cells

Results of the solar cell experiment of the first Brazilian satellite

N. Veissid*, P. Nubile, A.F. Beloto

Instituto Nacional de Pesquisas Espaciais, Laboratório de Materiais e Sensores, Av. dos Astronautas 1758, P.O. Box 515, CEP 12201-970, São José dos Campos, Brazil

Received 9 November 1995; revised 11 June 1996

Abstract

The first satellite of the Brazilian Complete Space Mission, launched on 9 February 1993, hosts a solar cell experiment (SCE). The objective of the SCE is to qualify in mission and real time the silicon solar cells for space use developed and manufactured in Brazil. The solar cells have the following characteristics: 4 cm^2 of area, base resistivity of 10 Ωcm and efficiency over 11% under AM0 condition. The SCE is a small solar module composed by a single array of six silicon solar cells connected in series, laid down in an aluminium mechanical structure. The signal generated by the array is sent to a peak detector circuit located inside the mechanical structure. Three telemetry signals are available for the SCE behavior analysis, which are the peak detector output, the temperature sensor output, located inside the SCE mechanical structure under the solar array, and the attitude sensor signal, which gives the sunlight incidence angle with respect to the SCE plane. The SCE signal versus temperature curve is used to obtain the solar cell current versus voltage characteristic parameters values, based on the double exponential model, using a computational method developed to accomplish this task in real time, during the satellite lifetime.

This work describes the solar cell experiment, the numerical methods and the analysis of the telemetry data received during the first two years in orbit. For this period, considering the standard deviation obtained in the output parameters, we can say that the radiation damage in the SCE solar cells is lower than expected when compared with data presented in the literature (1.7%) and those calculated from simulation in laboratory (1.0%). The analysis of the data indicates a degradation of the SCE solar cells around 0.5%.

Keywords: Solar cell experiment; Satellite; Radiation damage

* Corresponding author. Email: veissid@las.inpe.br

PII S0927-0248(96)00089-X

1. Introduction

Experiments conducted aboard satellites show the importance of the studies of simultaneous effects of thermal cycles, ionizing radiation damage, ultraviolet light and vacuum degradation on solar cells [1, 2]. The main reason is the extreme difficulty in simulating all these effects in laboratory, simultaneously.

The first satellite of the Brazilian Complete Space Mission, first space engine designed and constructed in Brazil is a meteorological data collection satellite (SCD1). It is a real time repeater of environmental data received by data collections platforms distributed along the Brazilian territory. The orbit is circular, 750 km high, with a period of 100 min, at an inclination of 25°. The rotation around its axis was 120 rpm, when first initiated into orbit, and now is approximately 60 rpm. The SCD1 is under illumination approximately 65 min and the rest of time it is in the shadow cone of the earth. Besides its main mission, the satellite SCD1 carries aboard the solar cell experiment (SCE), to test Brazilian silicon solar cells for space use. The satellite mechanical structure supports nine solar panels: one octagonal top panel and eight rectangular lateral panels. The SCE is located in the middle of one rectangular panel.

The literature reports solar cell experiments in satellites that work only to measure the short circuit current [2]. The SCE was developed to recover the full I–V characteristic based on the fitting of the telemetry signal with time orbit. A load resistance was shunted to the solar cell array terminal to set the operation around the maximum power voltage at the room temperature. As the satellite temperature varies during the orbit, we can obtain the voltage versus temperature curve of the SCE. It is possible to obtain the complete current by voltage characteristic of the solar cell by analysing this curve. The mathematical formalism is shown in this work.

This work describes the study, development and functional tests of the SCE. We also present the method to obtain the output parameters from telemetry signal and the analysis of the results.

2. Theoretical fundaments

The current versus voltage characteristic of a solar cell, represented by the double exponential model [3, 4], is given by

$$I = I_{\mathrm{L}} - I_{\mathrm{S1}}\left\{\exp\left[\frac{q(V + IR_{\mathrm{S}})}{kT}\right] - 1\right\} - I_{\mathrm{S2}}\left\{\exp\left[\frac{q(V + IR_{\mathrm{S}})}{2kT}\right] - 1\right\} - \frac{V + IR_{\mathrm{S}}}{R_{\mathrm{P}}}, \tag{1}$$

where I_{L} is the photogenerated current, I_{S1} and I_{S2} the saturation currents, R_{S} and R_{P}, the series and shunt resistances, T is the temperature, k is the Boltzman constant and V is the voltage at a given current I.

This equation has explicit and implicit temperature dependence. The saturation current dependence with temperature is found in the work of Wolf et al. [5] and it is

shown that

$$I_{Si} = C_{Si} T^{3/i} \exp\left(-\frac{E_g}{ikT}\right), \tag{2}$$

for $i = 1$ and 2. C_{S1} and C_{S2} are saturation current constants. The silicon gap energy as a function of temperature is given by [6]

$$E_g(T) = E_g(0) - \frac{\alpha T^2}{T + \beta}, \tag{3}$$

where $E_g(0) = 1.17$ eV, $\alpha = 0.473$ meV/K and $\beta = 636$ K.

The temperature dependence of the series resistance and photogenerated current can be approximated by

$$I_L(T) = I_L(T_{ref})[1 + CI_L(T - T_{ref})], \tag{4}$$

$$R_S(T) = R_S(T_{ref})[1 + CR_S(T - T_{ref}), \tag{5}$$

where CI_L and CR_S are proportionality constants and $T_{ref} = 25°C$ is the reference temperature to obtain the performance of solar cell. We consider no temperature dependence for the shunt resistance.

3. Solar cell experiment description

The SCE is composed of an array of six solar cells connected in series. Solar cells with $n^+/p/p^+$ structure were fabricated in 10 Ωcm, boron doped, 250 μm thick, ⟨1 0 0⟩ float-zone silicon. The n^+ was formed by 900°C $POCl_3$ diffusion which resulted in a junction depth of 0.3 μm. A 585 Å thick Ta_2O_5 antireflexive coating was applied by sputtering and Ti–Pd–Ag contacts were deposited on the front and back surfaces. Electrical connections between the cells were provided by home-made silver electrical interconnectors, 50 μm thick, with a geometric pattern designed to relieve thermal stress. The solar array is laid down on the external surface of an aluminium mechanical structure. The CMX cover glass from Pilkington has a borosilicate layer 150 μm thick, with 5% of cerium dioxide. SCE structure is shown in Fig. 1.

The design of the SCE had to take into account constraints and parameters given by the mission system group. No energy from the satellite power system was available to feed electrical circuits to process the experiment signal, the total SCE surface could not exceed 6×6 cm^2, three telemetry channels were allocated for monitoring the experiment and the maximum weight could not exceed 300 g.

A passive electrical circuit was developed to use only the electrical energy obtained from the conversion of the solar energy by its solar cells. This circuit, shown in Fig. 2, is accommodated inside the SCE mechanical structure. It transforms the near half sinusoidal module signal in a continuous signal, ranging from 0 to 5 V, suitable to be read by the satellite telemetry. A 30 Ω load resistance is used to polarize the string at near the maximum power point in the I–V characteristics.

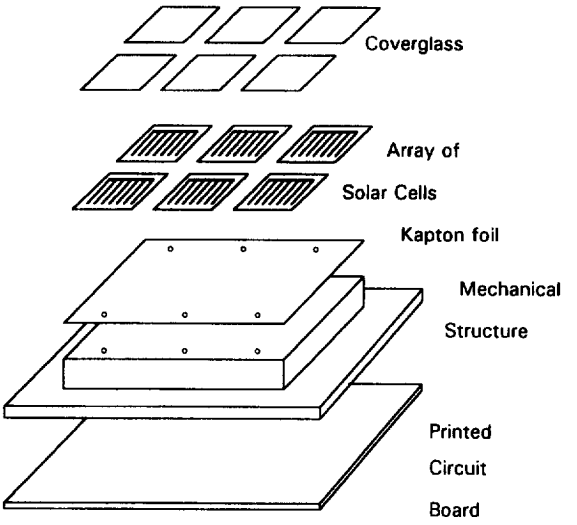

Fig. 1. Structural diagram of the solar cell experiment.

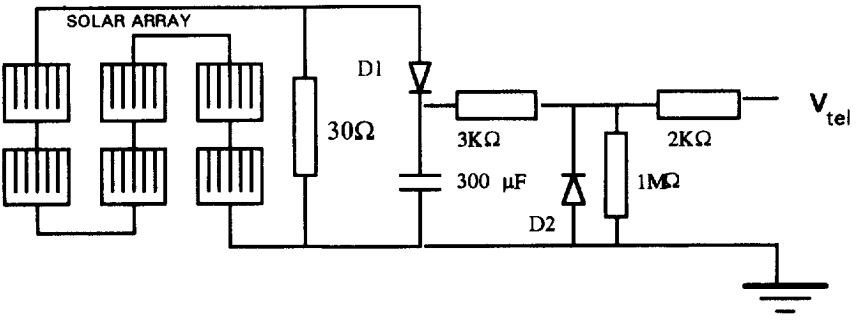

Fig. 2. Electrical circuit of the solar cell experiment.

The conditioning circuit consists of a peak detector, formed by the diode D1 and the 30 μF capacitance. The Schottky diode D1 (HP JANTX 1N5711) avoids quick capacitance discharge but the voltage drop on it has to be taken into account. The telemetry voltage has to be corrected to recover the true voltage value in the array output. The Schottky diode current–voltage characteristic obeys the analytical equation given by

$$I = C_{SCH} T^2 \exp\left(\frac{-q\phi_B}{kT}\right) \exp\left[\frac{q(V_D - IR_{SCH})}{kT} - 1\right], \tag{6}$$

where C_{SCH} is a constant, ϕ_B is the potential barrier and R_{SCH} is the diode series resistance. Using data given by the manufacturer, we can determine these parameter

using a fitting procedure of the $\ln(I/T^2) + qV_D/kT$ versus $1/kT$ plot. The calculated values for these parameters are: $C_{SCH} = 0.574\,\text{mA/K}^2$, $\phi_B = 0.612\,\text{eV}$ and $R_{SCH} = 80\,\Omega$.

The telemetry and peak detector impedances are both 1 MΩ, which gives an equivalent impedance, R_{eq} of 0.5 MΩ. The SCE voltage divided by this impedance is the current that flow through the diode. The temperature-dependent diode voltage is given by

$$V_D = \frac{kT}{q}\left\{1 + \ln\left(\frac{V_{tel}/R_{eq}}{CT^2 \exp(-\phi_B/kT)}\right)\right\} + R_S\frac{V_{tel}}{R_{eq}}. \tag{7}$$

4. Mathematical methods

The electrical signal of the SCE array (V_{array}) as function of the temperature of the solar cells considering that the I–V characteristic of all cells are identical, is given by

$$V_{array}(T) = R_L\left\{I_L(T) - I_{S1}(T)\left\{\exp\left[\frac{qV_{array}(T)}{6kT}\left(1 + \frac{6R_S(T)}{R_L}\right)\right] - 1\right\}\right.$$
$$\left. - I_{S2}\left\{\exp\left[\frac{qV_{array}(T)}{12kT}\left(1 + \frac{6R_S(T)}{R_L}\right)\right] - 1\right\} - \frac{V_{array}(T)}{6R_P}\left(1 + \frac{6R_S(T)}{R_L}\right)\right\}, \tag{8}$$

where R_L is the 30 Ω load resistance.

Using a numerical iterative fit of the V–T solar cell curve, it is possible to obtain the values of the fitted parameters. The telemetry voltage is the difference between the solar cell array voltage and the diode voltage ($V_{tel} = V_{array} - V_D$).

The method to fit the telemetry curve is a combination of the downhill and the minimum parabolic techniques. After several iterative processes, it is possible to obtain the values for the parameters that give the best fitting. These fitted parameters define the I–V curve of each solar cell in any illumination level and temperature.

The criterion chosen to obtain the best fitting is the minimization of the chi-square, given by

$$\chi^2 = \sum_{i=1}^{N}\left[\frac{(V_{tel})_i + (V_D)_i - V_{array}}{\sigma_V}\right]^2, \tag{9}$$

where N is the number of data points extracted from the voltage versus temperature curve. This criterion permits also to obtain the standard deviation of the fitted I–V curve parameters. The voltage standard deviation, σ_V, is a function of the analogical-to-digital converter of the satellite and it is approximately 20 mV.

When χ^2 is minimum, the variation δp of a parameter p, one of those present in Eq. (8), such as $\chi^2 = \chi^2_{min} + 1$ gives the standard deviation of this parameters [7].

By the error propagation theory we can obtain the standard deviations of the I–V curve output parameters short-circuit current, I_{SC}, open circuit voltage, V_{OC}, current at the maximum power point I_{MP}, voltage at the maximum power point, V_{MP}, efficiency

and fill factor. For example, Eq. (10) gives the standard deviation of the open circuit voltage:

$$\sigma_V^2 = \sigma_I^2\left(\frac{\partial V_{OC}}{\partial I_L}\right)^2 + \sigma_{I_1}^2\left(\frac{\partial V_{OC}}{\partial I_{S1}}\right)^2 + \sigma_{I_2}^2\left(\frac{\partial V_{OC}}{\partial I_{S2}}\right)^2, \tag{10}$$

where

$$\frac{\partial V_{OC}}{\partial I_L} = \frac{kT\exp\left(-\dfrac{V_{OC}}{2kT}\right)}{\sqrt{I_L I_{S1} + (I_{S2}/2)^2}}, \tag{11}$$

$$\frac{\partial V_{OC}}{\partial I_{S1}} = kT\exp\left(-\frac{V_{OC}}{2kT}\right)\left[\frac{I_{S2}}{I_{S1}^2} - \frac{I_L + I_{S2}^2/I_{S1}}{I_{S1}\sqrt{I_L I_{S1} + (I_{S2}/2)^2}}\right], \tag{12}$$

$$\frac{\partial V_{OC}}{\partial I_{S2}} = kT\exp\left(-\frac{V_{OC}}{2kT}\right)\left[\frac{I_{S2}/2}{\sqrt{I_L I_{S1} + (I_{S2}/2)^2}} - \frac{1}{I_{S1}}\right] \tag{13}$$

and

$$V_{OC} = 2kT\ln\{[\sqrt{I_L I_{S1} + (I_{S2}/2)^2} - I_{S2}/2]I_{S1}^{-1}\}. \tag{14}$$

To determine the solar cell I–V curve under the standard condition (AM0), the incident light power density has to be corrected considering the attitude angle, α, between the light incidence direction and the satellite rotation axis and the variation of the solar intensity due to seasonal variations on the earth–sun distance [4]. The incident power, P_{inc}, can be written as

$$P_{inc} = P_{SOLAR}\left\{1 + 0.0333\cos\left[\frac{(d-3)360^\circ}{365.25}\right]\right\}\sin\alpha, \tag{15}$$

where P_{SOLAR} is the solar irradiance, measured daily by the Earth Radiation Budget Satellite [8], and corrected for one astronomical unit; and d is the day of the year.

The corrected photogenerated current to the AM0 condition is given by

$$I_L[\text{AM0}] = I_L[\text{fitted}](135.3/P_{inc}). \tag{16}$$

5. Experimental results and analysis

We have performed I–V measurements in four solar cells at temperatures varying from 10°C to 70°C, with steps of around 10°C. The illuminated I–V curves were obtained for the AM0 condition (135 mW/cm^2) using a standard silicon solar cell as reference. The curves were treated to determine the best set parameters values of Eq. (1). Every experimental curve was fitted with the use of a computational routine, which applies alternatively the modified Gauss–Newton [13], downhill and parabolic

interpolation [7, p. 318] methods. This routine find the global minimum of the reduced chi-square, given by

$$\chi^2_{\text{red}} = \frac{1}{N - n_p} \sum_{i=1}^{N} \left[\frac{(I_{\text{exp}})_i - I(V_i)}{\sigma_1} \right]^2, \tag{17}$$

where σ_1 is the experimental accuracy of the measured current, I_{exp} is the measured current at V_i, I is the calculated current using Eq. (1), N is the number of points taken out of the I–V curve and n_p is the number of parameters of the analytical model. This method permits the determination of standard deviations of the fitted parameters values [10, 11].

The solar cells were irradiated with 5×10^{14} electrons/cm^2 at the energy of 1 MeV supplied by a dynamitron accelerator. The solar cells I–V characteristics were also measured after irradiation. With this study we verified that the analytical Eqs. (2)–(5) are acceptable even after irradiation [9].

Figs. 3–6 show the photogenerated current, saturation constants and series resistance as function of temperature, before and after irradiation. Table 1 shows the parameters values obtained from these curves for the representative solar cell.

The expected value for χ^2_{red} is around unity. In Table 1, the reduced chi-square of series resistance curves (see Fig. 6) and saturation current constants of J_{S1} and J_{S2} (see Figs. 4 and 5) indicate a reasonable fitting of these parameters. Higher χ^2_{red} values for the photogenerated current fitting (see Fig. 3) can be explained by the fluctuations of the solar simulator light beam, which are not considered in the standard deviation.

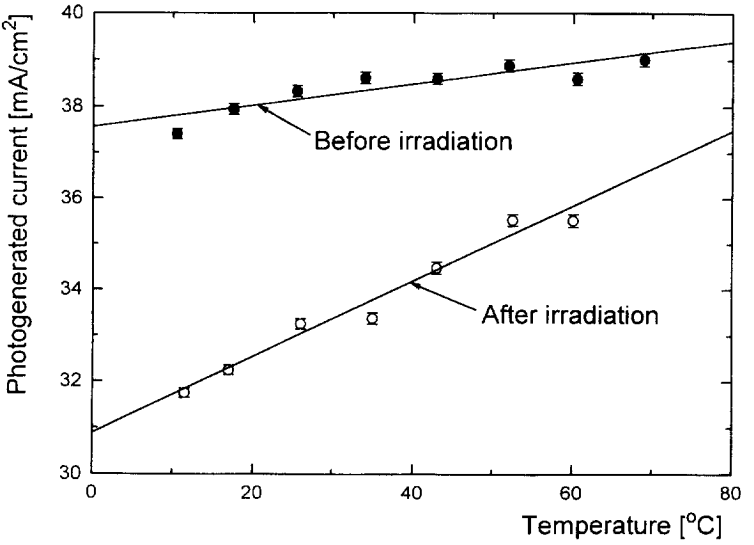

Fig. 3. Photogenerated current of the SCE representative solar cell.

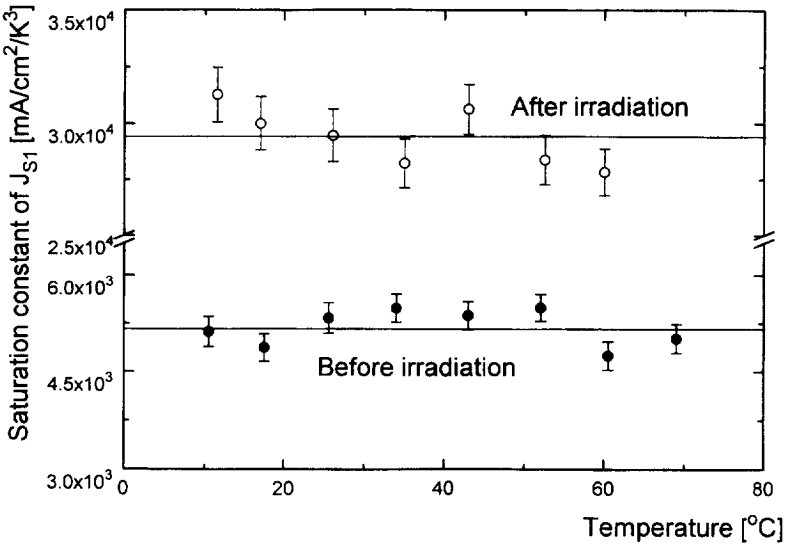

Fig. 4. Saturation constant of diffusion carrier process trough the depletion layer of the SCE representative solar cell.

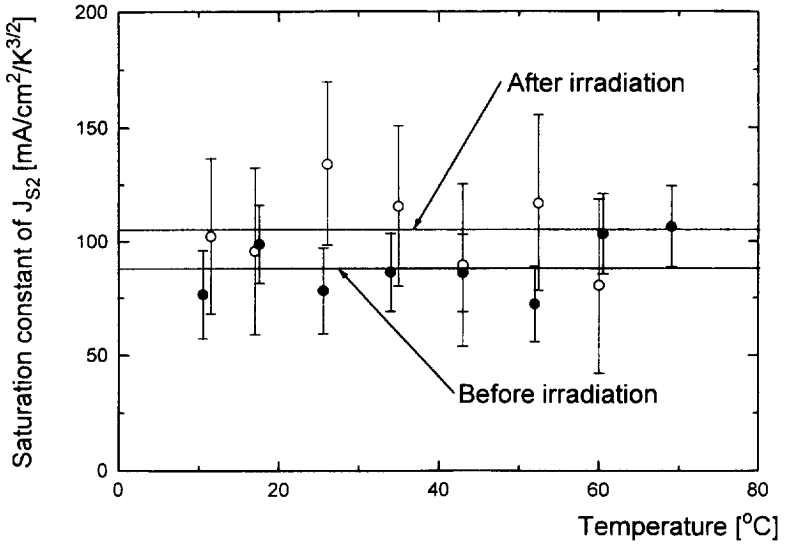

Fig. 5. Saturation constant of recombination-generated carrier process in the depletion layer of the SCE representative solar cell.

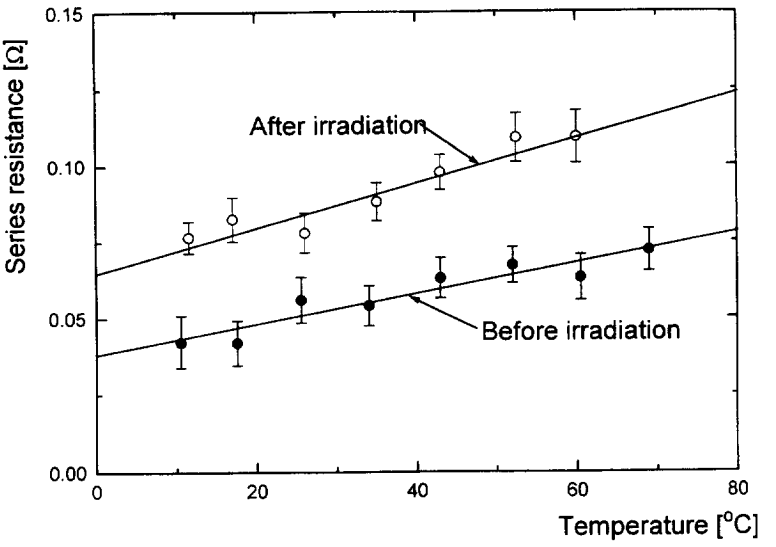

Fig. 6. Series resistance of the SCE representative solar cell.

Table 1
I–V Parameters of the I–V curve of the representative solar cell from lot

Eq.	Parameter	Before irradiation	After irradiation	Linearly interpolated to 750 days
5	I_L [25°C](mA)	150.09 ± 0.20	129.68 ± 0.19	149.42
	CI_L (%/°C)	0.0622 ± 0.0060	0.2504 ± 0.0082	0.0684
	χ^2_{red}	4.8	5.1	—
2	C_{S1} (mA/cm^2/K^3)	5180 ± 220	29320 ± 1040	5973
	χ^2_{red}	1.71	1.36	—
3	C_{S2} (mA/cm^2/K$^{3/2}$)	88.6 ± 17.7	105.2 ± 33.6	89.1
	χ^2_{red}	0.53	0.25	—
7	R_S [25°C] (mΩ)	50.6 ± 3.3	84.3 ± 2.7	51.7
	CR_S (%/°C)	1.01 ± 0.27	0.85 ± 0.19	1.00
	χ^2_{red}	0.34	0.46	—

Table 2 shows the parameter values for the SCE representative solar cell at reference temperature 25°C, before and after irradiation with 5×10^{14} e[1MeV]/cm^2, which is the equivalent fluence for 62.5 yr in the orbit of the SCD1 satellite. The third column value is obtained considering the values of Table 1 to the parameters calculated to 750 d.

Table 2
AM0 I–V curve output parameters values of SCE representative SC

Output parameter	Before irradiation	After irradiation	750 days in orbit simulating
I_{SC} (mA)	150.09	129.68	149.42
V_{OC} (mV)	554.52	508.60	551.06
I_{MAX} (mA)	139.52	120.66	138.96
V_{MAX} (mA)	465.53	422.33	462.53
Fill factor	0.780	0.773	0.781
Effic. (%)	12.18	9.56	12.06

5.1. SCE laboratory functional test

A laboratory test of the SCE was performed in a thermo-vacuum chamber. The solar cell array was illuminated through a window of the chamber at an intensity of 87 mW/cm^2, which simulated an illumination at an incident angle of 40° approximately. The voltage output as a function of the temperature, in the range of -30°C to $+40$°C was recorded and shown in Fig. 7, see curve *d*. Curve *b* shows numerical extrapolation of the functional test in the AM0 condition. It was not possible to realize experimentally this functional test in the AM0 illumination intensity, because the maximum value of the light intensity obtained inside the chamber was only 87 mW/cm^2. Curves *a* and *c* correspond to a numerical simulation of SCE considering an array similar to representative solar cell, where I–V characteristic parameters is given by Table 1, in the illumination angle of 90° and 40°, respectively.

Table 3 shows results for the I–V curve parameter fitting. The second column lists the mean values of direct measurements in the solar cells mounted in the SCE flight model.

5.2. Telemetry signal analysis

Daily telemetry data have been received every half second by earth stations located in São José dos Campos and Alcântara in Brazil, since the satellite was launched. Fig. 8 shows the data for the SCE output voltage and temperature obtained on 20 September 1994. On this day, the sun aspect angle was 68° and the spin satellite was 63.8 rotations per minute. The voltage drop when the satellite enters the shadow cone, observed in Fig. 8, is damped by the capacitor in the peak detector circuit.

The routine to extract the solar cell parameters of the SCE telemetry voltage has to consider the diode effect, discussed in Section 3, and albedo.

A rigorous analysis of the albedo effect in the satellite operation is very hard and unnecessary. To obtain a good approximation of it, we can consider that the earth is an uniform diffuse reflector with an albedo of 0.35, i.e., the earth reflects 35% of the light intensity from sun. The angle between the earth radius and the sunlight direction of the shadow cone output is 26.5°.

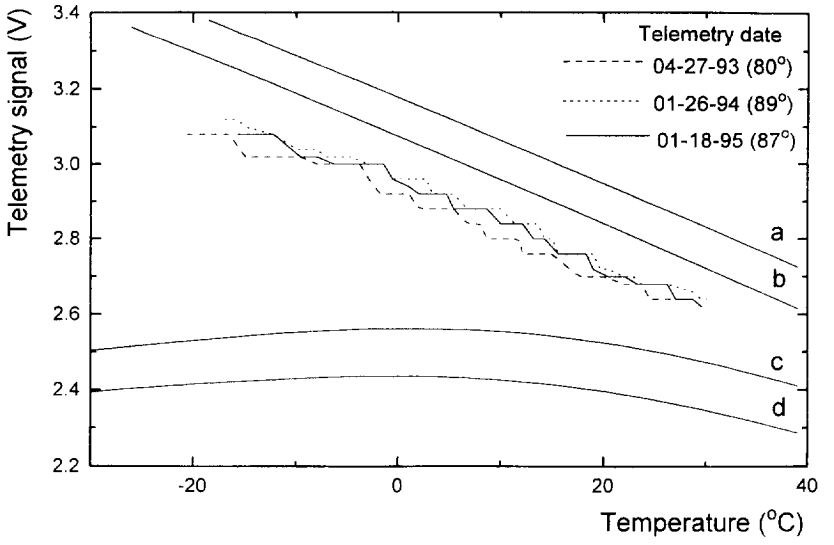

Fig. 7. Telemetry signal curves of the solar cell experiment.

Table 3
I–V curve output parameters values

Output parameter	Obtained from V–T curve fitting	Obtained from direct measurements	Obtained from SCE representative SC
I_{SC} (mA)	142.5	144.5 ± 5.1	150.1
V_{OC} (mV)	558.0	560.0 ± 11.4	554.5
I_{MAX} (mA)	131.0	133.2 ± 5.3	139.5
V_{MAX} (mA)	460.2	464.7 ± 11.3	465.5
Fill factor	0.758	0.765 ± 0.012	0.780
Effic. (%)	11.31	11.61 ± 0.69	12.18

Considering the simplified geometry given in Fig. 9, we calculated the light intensity as a function of time, considering $t = 0$ when the satellite leaves the shadow cone of earth. Table 4 indicates the values obtained in this calculation, where P is the fraction of AM0 intensity. The angles θ and γ indicate the satellite direction as a function of the sunlight normal and the position of the SCE in the maximum total light intensity, albedo and direct sunlight.

To exemplify the albedo effect, Fig. 10 shows the total light intensity for $t = 0$, 10 and 20 min and the albedo effect at the maximum light intensity in the SCE. The peak detector circuit of the SCE is sensitive only to the peak value in each satellite rotation. This value in function of temperature is used to fit the SCE V–T curve. Based on Fig. 10, we concluded that 10 min after exit from the shadow cone of the earth, the

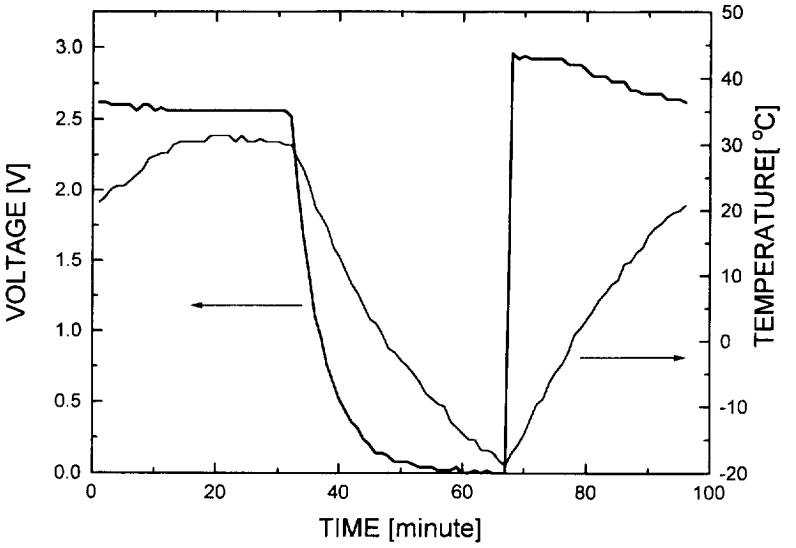

Fig. 8. SCE output voltage versus time for one orbit of SCD1 satellite.

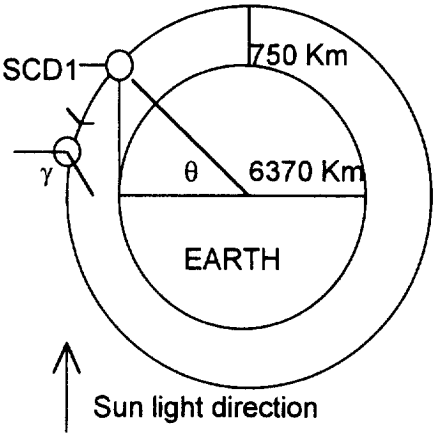

Fig. 9. Diagram of SCD1 orbit in relation of earth.

SCE peak detector sees only the direct sunlight intensity. An analogous conclusion is obtained when the SCE enters the shadow cone. Ten minutes before it, the SCE begins to see the albedo effect radiation. These parts of SCE signal received are not considered in the fitting of V–T curve.

The mathematical formalism, discussed in Section 4, is used for the fitting of each telemetry voltage versus temperature curve and to obtain the output I–V parameters

Table 4
Light intensity of SCE in function of output time of shadow cone of earth

θ(°)	26.5	19.3	12.1	4.9	−2.3	−9.5
T(min)	0	2	4	6	8	10
P(AM0)	1.198	1.163	1.126	1.087	1.046	1.003
γ(max)	105	106	108	109	110	110

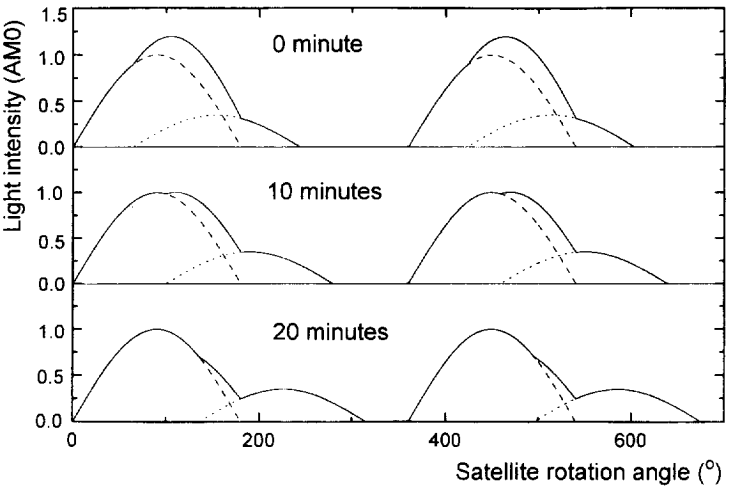

Fig. 10. Light intensity of SCE after the shadow cone of earth output.

standard deviations. Finally, to obtain the *I–V* parameters of the SCE solar cell the light intensity correction to the photogenerated current is made.

Several telemetry voltages per month were analyzed. Fig. 11 shows the results of these calculations for the energy conversion efficiency of the SCE solar cells. Each point represents the monthly parameter mean values, for the AM0 condition at 25°C. These points were calculated considering the standard deviations in its values, i.e. the inverse of the square standard deviations works as weights for obtaining these points.

These results show that after 2 yr the radiation effects were not able to change the solar cells performance significantly. We observed a decrease in the efficiency around 0.5%.

Fig. 11 shows the laboratory measurement curve made on the SCE representative solar cell, considering a linear variation with time in orbit of the values in first and third column of the Table 2. This figure also shows the efficiency of a conventional solar cell for space use analogous to the SCE solar cells. The data of the radiation

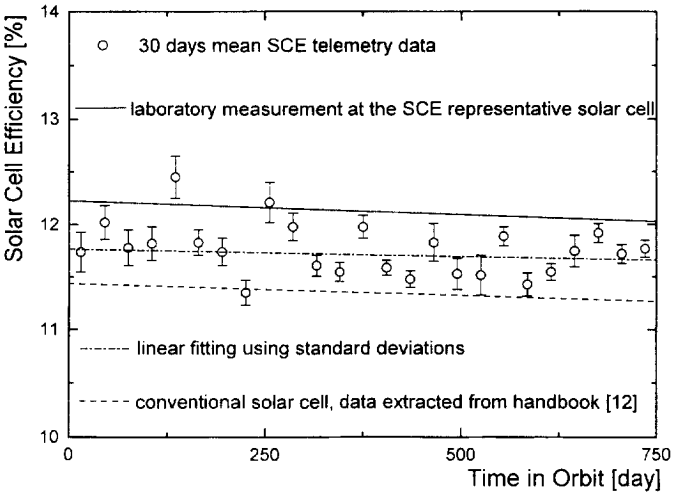

Fig. 11. Efficiency as a function of SCE time in orbit.

degradation was extracted from the literature from a solar cell similar to the SCE solar cell, i.e. the K4 solar cell (10 Ωcm) [[12], pp. 3–60]. The value adopted is the mean of 0.2 and 0.3 mm thickness of the K4 because the SCE solar cell is of 0.25 mm thickness.

5.3. *Heat flux analysis*

The sensor temperature is a thermistor (Pt 10 000) bounded inside the interior of the mechanical structure of the SCE. We had to be sure that the temperature read by the thermistor and the SCE module temperature were the same. The heat flow in the SCE was studied to solve this problem. We supposed a system with three layers of different materials: silicon, kapton foil and aluminum. The heat flux, Q_{heat}, that crosses the layers is the light power divided by π, because of the satellite spin. Eq. (8) indicates the temperature difference in each layer. Table 5 indicates the values obtained in this calculation, which indicate no significant differences between the temperature in the SCE array and the thermistor:

$$\Delta T_{mat} = Q_{heat} x_{mat}/k_{mat}, \tag{18}$$

where k_{mat} is the thermal conductivity.

We also considered the thermal inertia of the SCE. We calculated the time that a heat pulse spends to cross the layers, given approximately by $t \approx x_{mat}2/D_{eq}$, where D_{eq} is the equivalent thermal diffusivity. Using the values in Table 3, we calculated that the thermalization delay of the SCE was about 8 s. This delay does not influence the V–T values used to obtain the in-orbit solar cell parameters.

Table 5
Values of the thermal SCE study

	Silicon	Kapton foil	Aluminum
k_{mat} (W/cm/K)	1.28	0.00155	1.71
ρ (g/cm^3)	2.33	1.42	2.71
C (J/g/K)	0.75	1.09	0.96
x (mm)	0.3	0.2	3.0
ΔT_{mat}(K)	0.001	0.56	0.008

6. Conclusion

This work shows the feasibility of low cost, highly reliable, solar cells performance experiments aboard low orbit satellites. The problems posed by spin and variable temperature effects can be corrected using a simple electrical conditioning circuit and a mathematical approach capable to make all the corrections and fittings.

The parameters obtained from the fitted SCE signal versus temperature curve agree satisfactorily with the I–V curve parameters obtained by direct measurements. For the first time, it is demonstrated that a low-cost experiment with a passive electric circuit can be used to obtain the complete I–V solar cells curves during the satellite mission lifetime.

After 2 yr of the satellite launching, the efficiency derived of the data analysis decreased around 0.5%. This value is comparable to its standard deviation. Nevertheless, these data qualify the lay down and bonding procedures used in the SCE fabrication.

Acknowledgements

The authors wish to express their sincere thanks to the Laboratório de Microeletrônica of the São Paulo University (LME/USP) for the use of their facilities and IPEN/CNEN for their helpful assistance in the samples electron irradiation. Dr. Nelson Veissid is grateful to Conselho Nacional de Pesquisas (CNP_q/BRAZIL), process number 301106/90-8. The authors wish to thank Mr. Rogério Ramos Bastos Miguez for all telemetry reports.

References

[1] D.H. Walker and R.L. Statler, Solar Cells 23 (1988) 245.
[2] C. Huang, Q. Wang and Q. Jiang, Proc. Eighteenth IEEE Phot. Spec. Conf., Las Vegas (1985) p. 634.
[3] H.J. Hovel, in: Semiconductors and Semimetals, Vol. 11, Eds. R.K. Willardson and A.C. Beer (Academic Press, New York, 1976).
[4] H.S. Rauschenbach, Solar Cell Array Design Handbook, (Van Nostrand Reinhold Company, New York, 1980).

[5] M. Wolf, G.T. Noel and R.J. Stirn, IEEE Trans. Electron Dev. ED-24 (1977) 419.
[6] M.S. Sze, Physics of Semiconductor Devices, (Wiley, New York, 1981).
[7] W.H. Press et al., Numerical Recipes in Pascal, (Cambridge University Press, Cambridge, 1992).
[8] R.B. Lee, Solar Geophysical Data Comprehensive Reports, 607 (Part II) (March 1995) p. 32.
[9] N. Veissid, P. Nubile, A.F. Beloto and A.M. de Andrade, Proc. 21 Specialists Photovoltaic Conf. Kissimie, FL, USA (1990) p. 1184.
[10] N. Veissid and A.M. Andrade, Proc. 10 E.C. Photovoltaic Solar Energy Conf. Lisbon-Portugal (1991) p. 43.
[11] N. Veissid, D. Bonnet and H. Richter, Solid-StateElectron. 38 (11) (1995) 1937.
[12] H.Y. Tada et al., Solar Cell Radiation Handbook, Jet Propulsion Laboratory, (California Institute of Technology, Pasadena, California, 1982).
[13] H.O. Hartley, Technometrics 32 (1961) 261.